

An alignment approach for coupling mounts using a fiber ended micro-lens

SHUPING LI, JINGPING ZHU, WANGUANG QIN*, YAOHUI CHEN

Key Laboratory for Physical Electronics and Devices of the Ministry of Education and Shaanxi Key Laboratory of Information Photonic Technique, Xi'an Jiaotong University, Xi'an, 710049, China

The direct butt-coupling technique for fiber–chip coupling yields a 7–10 dB power loss because of the unequal spot-sizes associated with each device. We design a fiber ended micro-lens to enhance the coupling efficiency and further derive the meridian expression. To meet the needs of the sub-micron alignment tolerance, a self-aligned mounting is developed, and electro-strictive actuators are employed. Along with the reference alignment solution, alignment feedback and control can be realized.

(Received July 5, 2011; accepted July 25, 2011)

Keywords: Self-aligned mounting, Butt coupling, Alignment, Electro-strictive actuators

1. Introduction

The cost of photonic device packaging is about 80 % that of the integrated module. A large proportion of the cost originates from the process of achieving accurate alignment. This is one of the largest barriers to mass production. Highly efficient coupling techniques are a critical requirement for optoelectronics industry.

When a single mode fiber is directly butt-coupled to a photonic device, there is a 7–10 dB power loss and submicron alignment tolerances are required. To achieve both low coupling loss and large alignment tolerances, it is necessary to transform the mode on chip to better match that of the fiber. Using this concept, various integrated mode transformer solutions have been proposed. However, most of these approaches still involve complex growth and processing steps. Micro-lenses which are fabricated directly on the end faces of single-mode fibers (SMFs) have been used because they can produce high coupling efficiencies, and expand the alignment tolerance of the system [1,2]. In this paper, we propose a novel fiber-ended micro-lens (FEML) and derive its meridian expression. Then, we focus on packaging technology accurate alignment in mass production. High-precision passive fiber-to-integrated-optical-device coupling methods have been introduced which use silicon as a substrate and grooves or oversized rib waveguides as self-alignment mounting markers [3-5].

During the last decade, ultra-precision machining and small motors, the high resolution and stiffness were required for high-precision optical coupling. However, the conventional displacement transducers present serious problems for precision positioning because of mechanical backlash and generative force. In addition, generative force affects the response speed. This has accelerated the development of electric-field-induced strain ceramic actuators. New materials, such as lead zirconate titanate (PZT) based and lead-magnesium-niobate (PMN) based

ceramics have been demonstrated to have excellent actuator characteristics.

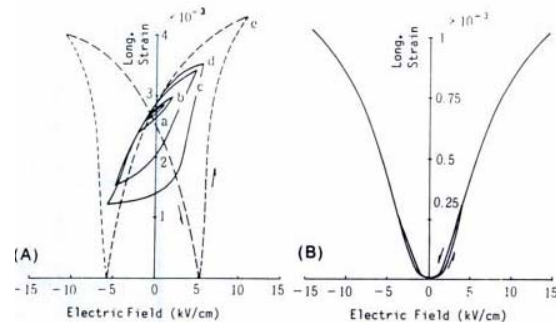


Fig. 1. (A) Field-induced strains in piezoelectric PLZT (7/62/38) and (B) in an electro-strictive PMN-based ceramic (0.9PMN-0.1PT).

Fig. 1 shows strain curves for PZT and 0.9Pb(Mg_{1/3}Nb_{2/3})O₃-0.1PbTiO₃ at room temperature [6]. The physical properties of these electro-strictive materials, such as high response speeds and high electro-strictive strain behavior, have identified them as some of the most attractive materials for the fabrication of smart material actuators. The electro-strictive actuators (ESAs) can create displacements of several tens of micrometers with a high accuracy ($\pm 0.01 \mu\text{m}$) and high response speed ($\approx 10 \mu\text{s}$). Therefore, the ESAs have been applied as actuators in many micro-electromechanical systems (MEMS).

In this paper, ESAs were applied in a passive coupling method. Self-alignment ribs on a silicon substrate were used for rough alignment. The ESAs were used for accurate adjustment along the transverse and longitudinal directions to optimize the coupling efficiency. Electrical-control and feedback circuits embedded in the silicon substrate. Such an alignment approach meets the standards

from other coupling methods, and the technical requirements for coupling using FEML. It allows for a pluggable, compact and semi-automatic coupling process.

2. Micro-lens coupling simulation

A main problem in fiber and waveguide coupling is the mode mismatch, the fiber micro-lens is applied. The mode of the fiber can be approximated by a Gaussian beam [7]. The Fresnel reflections from the end-faces of the fiber and the chip can be ignored. The transmitted light through the micro-lens surface boundary is a scalar of the Gaussian beam. Finally, at the edge of waveguide, mode coupling happens, and the critical mode mismatch loss level can be determined.

The geometric profile of the micro-lens for this coupling configuration (Fig. 2) is given by [8]:

$$z(r) = \frac{\sqrt{(n-1)^2 f^2 + (n^2-1)^2 r^2}}{(n^2-1)} - \frac{f}{n+1} \quad (1)$$

where, f is the theoretical focal length of micro-lens, n is the refractive index of micro-lens material ($n=1.46$), r is the variable along the transverse dimension, and z is the variable along the longitudinal dimension.

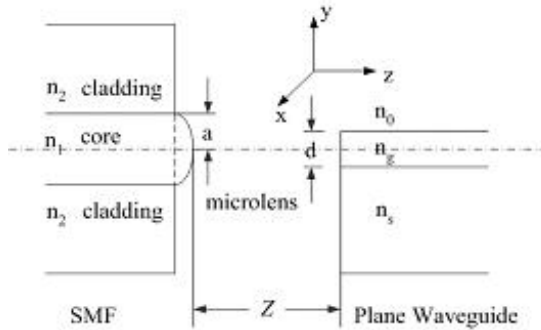


Fig. 2. Schematic of the coupling system comprising the fiber and planar waveguide.

The material refractive index of the single mode fiber core and cladding are 1.46527 and 1.46, respectively, and the radii of the core and cladding are $4.15\mu\text{m}$ and $62.5\mu\text{m}$, respectively, and the mode radius is $5.06\mu\text{m}$. And the refractive index of core and substrate of LiNbO_3 planar waveguide are 2.148 and 2.138, respectively, and the depth of the core is $5\mu\text{m}$. In this case, when $Z=f=9\mu\text{m}$, low-loss coupling can be achieved by optimizing the overlap integral between the waveguide mode and the optical fiber mode. The minimum mode mismatch loss was estimated to be 0.698 dB. This includes the mode conversion loss from the boundary of micro-lens, which was 0.153 dB. The theoretical coupling efficiency can be as large as 82.2%. Average coupling efficiencies of 61.0% and 80.2% were estimated at the transverse and longitudinal alignment tolerances of $\pm 1\mu\text{m}$ from the optimal position.

Furthermore, we employed commercial software to simulate the propagation of the light from the fiber coupling to the slab waveguide (Fig. 3). And focal length of the micro-lens is $9\mu\text{m}$, and the end-face of the slab waveguide located in the position of $z=52\mu\text{m}$. A mesh of $0.01\mu\text{m}$ by $0.01\mu\text{m}$ was used in the transverse-longitudinal plane. A minimum power loss of 1.04 dB was estimated.

The variations in the normalized output power with position along the y and z directions are shown in Fig. 4. This demonstrates the need for strict alignment tolerance requirements. The maximum coupling efficiency is 0.71 for alignment in the y -direction. However, when the displacement is 0.5 and $1\mu\text{m}$ along the y direction, the corresponding coupling efficiencies are 0.61 and 0.43, respectively. Coupling systems for fibers to slab waveguides require a fiber alignment accuracy of $< 0.5\mu\text{m}$ in the y -direction. However, they have larger tolerances in the x and z directions. Therefore, we can infer the coupling systems for fibers to strip waveguides require fiber alignment accuracies of $< 0.5\mu\text{m}$ in both the y and x directions. These requirements motivated our efforts to develop the ESA technique described below. Moreover, the concepts discussed above will be useful to develop similar techniques in the future. This simulation process has defined the basic problem that must be solved and has provided new data for ESAs structure design.

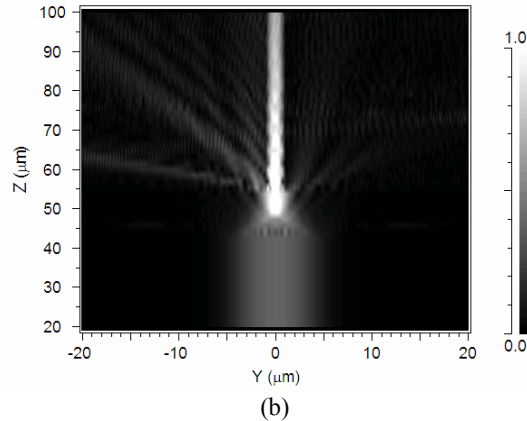
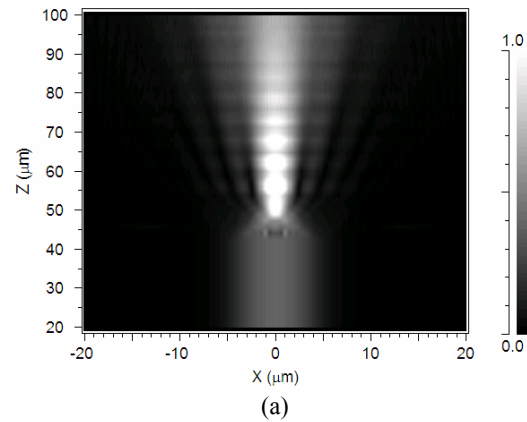


Fig. 3. Propagation of light in the (a) xoz and (b) $yozy$ planes.

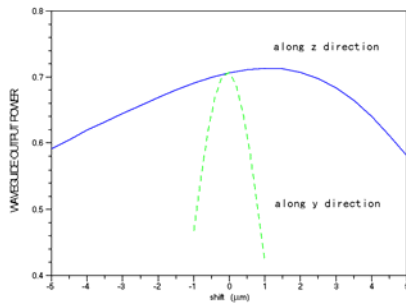


Fig. 4. Coupling efficiency as a function of position in the y and z directions.

3. Self-aligned mounting

The V-groove structure for fiber alignment on the waveguide substrate is shown in Fig. 5. This technique has shown promise for coupling alignment. However, the dimensional stability of the etched structure depends strongly on the parallel alignment of the etch mask and the crystal lattice of the wafer. Commercially available wafers have are flat to a maximum accuracy of 0.3° (in a normal distribution) as measured using x-ray or laser techniques. With an uncertainty of $\pm 0.5^\circ$ between crystal axis and the v-groove, the error in the groove width is about $1 \mu\text{m}$. Misalignment of the structure to the crystal axis leads to more complex and accurate requirements in during the fabrication process. This will greatly increase the cost, and make mass production impossible to realize. For the alignment process, precise exterior alignment tests and motorized instruments are still essential.

We adopted a structure in our system as shown in Fig. 5. We used the groove as a rough alignment and mounting structure with a micron or greater tolerance. High precision alignment and mounting functions are then accomplished by ESAs (Fig. 5). The V-groove is fabricated using a wet chemical etching step with a solution of citric acid and hydrogen peroxide. The saw is fabricated by simple micromachining technology or standard photolithography in the Si substrate. And then the ESAs are glued into the saw using epoxy exhibition shrinkage. This structure can also be customized for other applications.

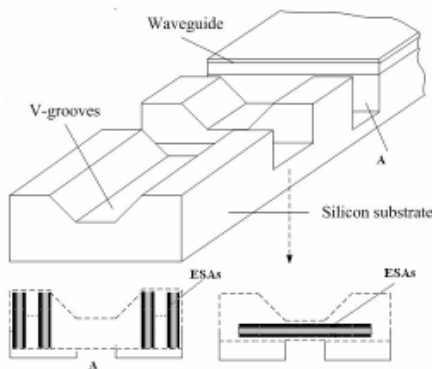


Fig. 5. Schematic of the etched V-groove structure.

4. Electro-strictive actuators

The piezoelectric ceramic actuator (PCA) is an ESA. Typical PCAs are multilayer elements. PCAs are preferable for actuation of less than several hundred microns. They offer lower power consumption and in a more compact package than other electromagnetic drive actuators. Moreover, ESAs have large dynamic ranges and small minimum adjustment step sizes. For example, for an actuator that is $9 \times 2 \times 3 \text{ mm}$, a $6.6 \mu\text{m}$ free displacement can be obtained [9]. Therefore, we designed a prototype with this type of ESA (Fig. 6). In the future, for this application more complex ESAs would be preferred, but better fabrication techniques and further experiments are required. The transverse adjustment could be performed in such way to provide better sub-micron alignment. Cluster A can be customized to serve as a stable transverse mounting structure in addition to performing alignment.

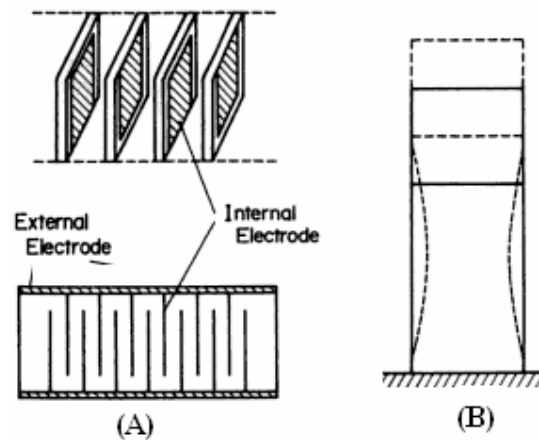


Fig. 6. Structure of the piezoelectric ceramic actuator.

For the butt-join coupling between a single mode fiber and a slab waveguide, as the opening angle of the v-groove is defined by the crystal orientation the vertical position of the fiber is defined by the width of the v-groove on the substrate surface only. And the error in the groove width should be brought about $1 \mu\text{m}$ in during the V-groove fabrication process. At meantime, the tolerances in the cladding diameter and the eccentricity of the core of the fiber have to be considered. The tolerance in the cladding diameter is about $\pm 1 \mu\text{m}$, and the coating layer will bring the tolerance of $\pm 10 \mu\text{m}$. The maximum total tolerances reach above $12 \mu\text{m}$. These tolerances of passive alignment can be corrected using the ESAs. The ESA (La: PZT) used for the experiment has a nominal maximum expansion of $12\text{-}15 \mu\text{m}$ under input voltage from 0 to 300V, and the response time is lower than 1 ms.

To achieve the best coupling efficiency, reference coordinates and related control parameters were obtained both from the simulation data (Fig. 4) and the experiment. In addition, aging and temperature were considered. Internal sensor feedback for all of the alignment functions can be performed on the chip itself. Although accurate

optical sources and test instruments are still essential for more accurate alignment, external feedback test data can be treated as an alternative to the default internal alignment solution. Combined with a passive fiber connector with a millimeter-scale alignment tolerance, the ESA structure can be customized to serve as a micro fiber motion instrument as well. Because electrical control is a mature technique, all functions listed above can be abstracted as functions of the electrical feedback and control signal. With an embedded optimal alignment algorithm in the control IC, both automatic and manual alignment should be more simple and practical when performed by the system on the chip.

5. Conclusions

In this work, we propose an alignment coupling mounting based on Si V-groove technology and electrostrictive actuators. The mounting is realized using only the standard photolithography and wet chemical etching techniques. Combined with proper mounting structures on the silicon substrate, fiber-chip coupling can be accomplished by systems located on the chip itself. At meantime, the electrostrictive actuators (ESAs) can create displacements of several tens of micrometers with a high accuracy of $\pm 0.01 \mu\text{m}$, these technologies make accurate alignment possible with integrated pluggable self-alignment units. As the fiber-chip alignment tolerance volume increases, the average cost of such integrated alignment structures will be less than other passive alignment methods with the same precision. This innovation is necessary for the future design and manufacture of photonic devices.

References

- [1] M. Galarza, K. De Mesel, D. Fuentes, et al. *Appl. Phys. B*, **73**, 585 (2001).
- [2] F. Schiappelli, R. Kumar, M. Prasciolu et al., *Microelectronic Engineering*, **73-74**, 397 (2004).
- [3] T. S. Barry, D. L. Rode, M. H. Cordaro, et al., *IEEE Transactions On Components, Packaging, And Manufacturing Technology-Part B*, **18**, 685 (1995).
- [4] T. Sterkenburgh, H. Franke, M. Becker, M. Garen, *Appl. Phys. B*, **68**, 1061 (1999).
- [5] R. Hauffe, U. Siebel, K. Pertermann, et al., *IEEE Transactions On Advanced Packaging*, **24**, 450 (2001).
- [6] K. Uchino. Electrostrictive actuators: materials and applications. In: Rosed CZ et al., editors. *Piezoelectricity*, 331-6 (1992).
- [7] C. W. Barnard, J. W. Y. Lit, *Appl. Optics*, **32**, 2090 (1993).
- [8] J. P. Zhu, T. T. Tang, X. Hou, *SPIE*, 3551, 163 (1998).
- [9] S. Takahashi, Longitudinal mode multilayer piezoceramic actuators, *Am. Ceram. Soc. Bull.*, **63**, 1156 (1986).

*Corresponding author: wgqin2@126.com